CHEMICAL EVOLUTION AND ESTIMATED FLOW VELOCITY OF WATER IN THE TRINITY AQUIFER, SOUTH-CENTRAL TEXAS

U.S. GEOLOGICAL SURVEY
Water-Resources Investigations Report 97–4078

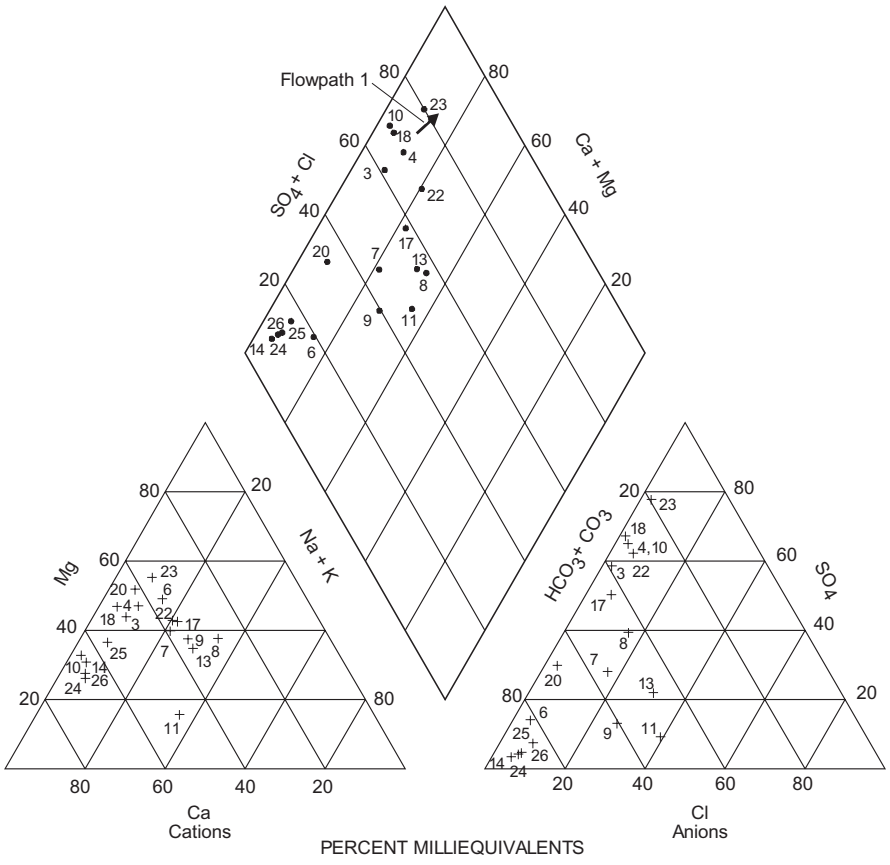

A contribution of the
Regional Aquifer-System Analysis Program

USGS
science for a changing world

CHEMICAL EVOLUTION AND ESTIMATED FLOW VELOCITY OF WATER IN THE TRINITY AQUIFER, SOUTH-CENTRAL TEXAS

By S.A. Jones, Roger W. Lee, and John F. Busby

U.S. GEOLOGICAL SURVEY
Water-Resources Investigations Report 97–4078

Austin, Texas
1997

U.S. DEPARTMENT OF THE INTERIOR

BRUCE BABBITT, Secretary

U.S. GEOLOGICAL SURVEY

Gordon P. Eaton, Acting Director

For additional information write to:

District Chief
U.S. Geological Survey
8011 Cameron Rd.
Austin, TX 78754–3898

Copies of this report can be purchased from:

U.S. Geological Survey
Branch of Information Services
Box 25286
Denver, CO 80225–0286

CONTENTS

FIGURES

TABLES

VERTICAL DATUM AND ISOTOPIC UNIT EXPLANATIONS

Sea level: In this report, "sea level" refers to the National Geodetic Vertical Datum of 1929—a geodetic datum derived from a general adjustment of the first-order level nets of both the United States and Canada formerly called Sea-Level Datum of 1929.

Isotopic Unit Explanations:

Per mil: A unit expressing the ratio of stable-isotopic abundances of an element in a sample to those of a standard material. Per mil units are equivalent to parts per thousand. Stable-isotopic ratios are computed as follows:

$$\delta X = \left(\frac{R(sample)}{R(standard)} - 1\right) \times 1{,}000 \ ,$$

where

δ represents the "del" notation,

X represents the heavier stable isotope, and

R is the ratio of the heavier stable isotope to the lighter stable isotope in a sample or standard.

The δ values for stable-isotopic ratios discussed in this report are referenced to the following standard materials:

Element	R	Standard identity and reference
carbon	carbon-13/carbon-12 ($\delta^{13}C$)	Pee Dee Belemnite (PDB) (Fritz and Fontes, 1980, p. 14)
carbon	carbon-14/carbon-12 (^{14}C)	National Bureau of Standards, 1980 oxalic acid standard (Fritz and Fontes, 1980, p. 14)
hydrogen	hydrogen-2/hydrogen-1 or deuterium/protium (δD)	Vienna-Standard Mean Ocean Water (Fritz and Fontes, 1980, p. 13)
oxygen	oxygen-18/oxygen-16 ($\delta^{18}O$)	Vienna-Standard Mean Ocean Water (Fritz and Fontes, 1980, p. 11)
sulfur	sulfur-34/sulfur-32 ($\delta^{34}S$)	Cañon Diablo Troilite (CDT) (Fritz and Fontes, 1980, p. 16)

Chemical Evolution and Estimated Flow Velocity of Water in the Trinity Aquifer, South-Central Texas

By S.A. Jones, Roger W. Lee, *and* John F. Busby

Abstract

Three permeable zones with varying lithology and water chemistry compose the Trinity aquifer, a principal source of water in the 5,500-square-mile study area in south-central Texas. The upper permeable zone locally yields small quantities of water to wells and was not included in this study. The middle permeable zone primarily is composed of limestone with minor amounts of dolostone. Terrigenous sand and marine limestone, with minor amounts of dolostone, are the principal lithologic units in the lower permeable zone. Dissolved solids concentrations range from 329 to 1,820 milligrams per liter in water samples from the middle permeable zone and from 518 to 3,030 milligrams per liter in water samples from the lower permeable zone. Principal hydrochemical facies in the middle permeable zone are calcium magnesium bicarbonate and calcium magnesium sulfate. Hydrochemical facies in ground-water samples from the lower permeable zone vary. Tritium concentrations as large as 5.3 tritium units in the southeastern part of the study area are indicative of relatively recent recharge. Results of a geochemical mass balance simulation along a flowpath in the middle permeable zone indicate a mass transfer of 4.25 millimoles per liter of dolomite dissolved, 5.74 millimoles per liter of gypsum dissolved, 0.46 millimole per liter of sodium chloride dissolved, 8.07 millimoles per liter of calcite precipitated, and 0.67 millimole per liter of calcium-for-sodium cation exchange between solid and aqueous phases. These results support dedolomitization as a principal chemical process in the middle permeable zone of the Trinity aquifer. Results of a simulation along a flowpath in the lower permeable zone indicate a mass transfer of 0.41 millimole per liter of dolomite dissolved, 0.001 millimole per liter of gypsum dissolved, 9.58 millimoles per liter of sodium chloride dissolved, 1.09 millimoles per liter of calcite precipitated, and 1.11 millimoles per liter of sodium-for-calcium cation exchange between solid and aqueous phases. Lower permeable zone processes indicate sodium chloride dissolution, dedolomitization, and cation exchange. Ground-water-flow velocities determined from adjusted carbon-14 ages, calculated using NETPATH, for selected flowpaths in the middle and lower permeable zones were about 1.7 feet per year and less than about 4.4 feet per year, respectively.

INTRODUCTION

The Trinity aquifer study was a part of the Edwards-Trinity Regional Aquifer-System Analysis (RASA). During 1978–94, the RASA program of the U.S. Geological Survey (USGS) studied 25 regional aquifer systems that supply appreciable amounts of ground water to large parts of the Nation. The overall objectives of each RASA project were to describe the ground-water-flow system, describe the geology, hydrology, and geochemistry, and integrate results of previous studies to form a comprehensive base of information relating to each system (Sun, 1986; Barker and Ardis, 1992).

During 1990–93, the USGS studied the geochemistry of the Trinity aquifer in south-central Texas to characterize chemical evolution that occurs as water moves from areas of recharge to areas of discharge and to estimate the velocity of ground-water flow. The purpose of this report is to document the methods and results of the study. Carbonate rock cores from four

locations in the aquifer were analyzed to determine mineralogy, petrology, and bulk rock composition. Water samples were collected from 26 wells in the Trinity aquifer. The results of the mineral and water analyses were used to determine rock-water interactions in the aquifer. The laboratory results and interactions were used to constrain mass-transfer models for two selected flowpaths. The models estimate carbon exchange among rock, water, and atmosphere and provide adjusted carbon-14 (^{14}C) content for water as it traverses a flowpath. Subsequent calculations of travel time and distance between wells were used to determine ground-water velocity along each flowpath.

The study area comprises approximately 5,500 square miles (mi^2) of south-central Texas (fig. 1). The area, coincident with much of the region known locally as the Hill Country, includes the southeastern edge of the Edwards Plateau and extends southeastward to the Balcones fault zone. The study area also is coincident with the northern parts of the Nueces, San Antonio, and Guadalupe River Basins. In the western part of the study area (Nueces River Basin), streamflow generally is to the south; in the central part of the study area (San Antonio River Basin), streamflow generally is to the southeast; and in the eastern part of the study area (Guadalupe River Basin), streamflow generally is to the east. The area is sparsely populated and much of the land is used for ranching. The climate is subhumid to subarid with average annual precipitation ranging from 25 to 35 inches per year (in/yr) (Ashworth, 1983).

Geologic Setting

The rocks that form the Trinity aquifer were deposited during the Early Cretaceous Period over eroded Paleozoic rock (Barker and Ardis, 1992). Stratigraphically, the rocks are divided, from oldest to youngest, into the Hosston and Sligo Formations, Hammett Shale, Cow Creek Limestone, Hensel Sand, and Glen Rose Limestone (fig. 2). Erosion has removed most of the overlying Edwards Group rocks (Rose, 1972), which cap some hilltops in the study area. The rocks of the Trinity aquifer were deposited during the northwest transgression of a warm, shallow sea on a gently inclined carbonate platform. Three transgressive-regressive cycles resulted in three time-stratigraphic subunits (Amsbury, 1974). The first subunit comprises the Hosston and Sligo Formations. The second comprises the Hammett Shale and the Cow Creek Limestone; and the third, the Hensel Sand and the Glen Rose Limestone.

The Stuart City reef trend, an almost continuous reef island ridge along the seaward edge of the continental shelf, developed as the Glen Rose Limestone was being deposited. The reef structure served as a barrier between the high-energy sea and the more tranquil backwaters behind the reef. This restriction produced ideal conditions for deposition of the evaporites in the upper Glen Rose Limestone (Stricklin and others, 1971).

Structurally, the study area is bounded by the Llano uplift to the north, the Balcones fault zone and San Marcos arch to the south and east, and the Edwards Plateau to the west (fig. 3). These features, combined with the southeasterly regional dip and the uneven pre-Cretaceous surface, affect the hydrogeology and ground-water flow in the area.

The Llano uplift was a topographic high during the Cretaceous Period. Sediments deposited during Early Cretaceous time thin northward as they approach the uplift. The Balcones fault zone is a series of southwest-to-northeast-oriented normal faults that can restrict or enhance ground-water flow. The San Marcos arch is a buried structural feature associated with the Llano uplift. The units that compose the Trinity aquifer thin as they cross the southeastward-plunging axis of the San Marcos arch.

Hydrogeologic Characteristics

Ground-water movement in the aquifer generally follows the regional dip of the rocks toward the south and southeast at approximately right angles to potentiometric-surface contours (fig. 1). The regional dip of the rocks is 10 to 15 feet per mile (ft/mi) in the north and northeastern part of the study area and increases to 100 ft/mi at the southern limit of the study area in the Balcones fault zone (Ashworth, 1983). Because the Hosston and Sligo Formations were deposited on an uneven Paleozoic surface (Barker and Ardis, 1992), the thickness of the unit varies. The presence of caverns in the Glen Rose Limestone can have a marked effect on ground-water-flow direction and velocity locally (Hammond, 1984). Units in the Trinity aquifer are complex with significant vertical and lateral heterogeneities in permeability (E.L. Kuniansky, U.S. Geological Survey, written commun., 1994).

The Trinity aquifer is divided into three water-yielding zones—the upper, middle, and lower Trinity

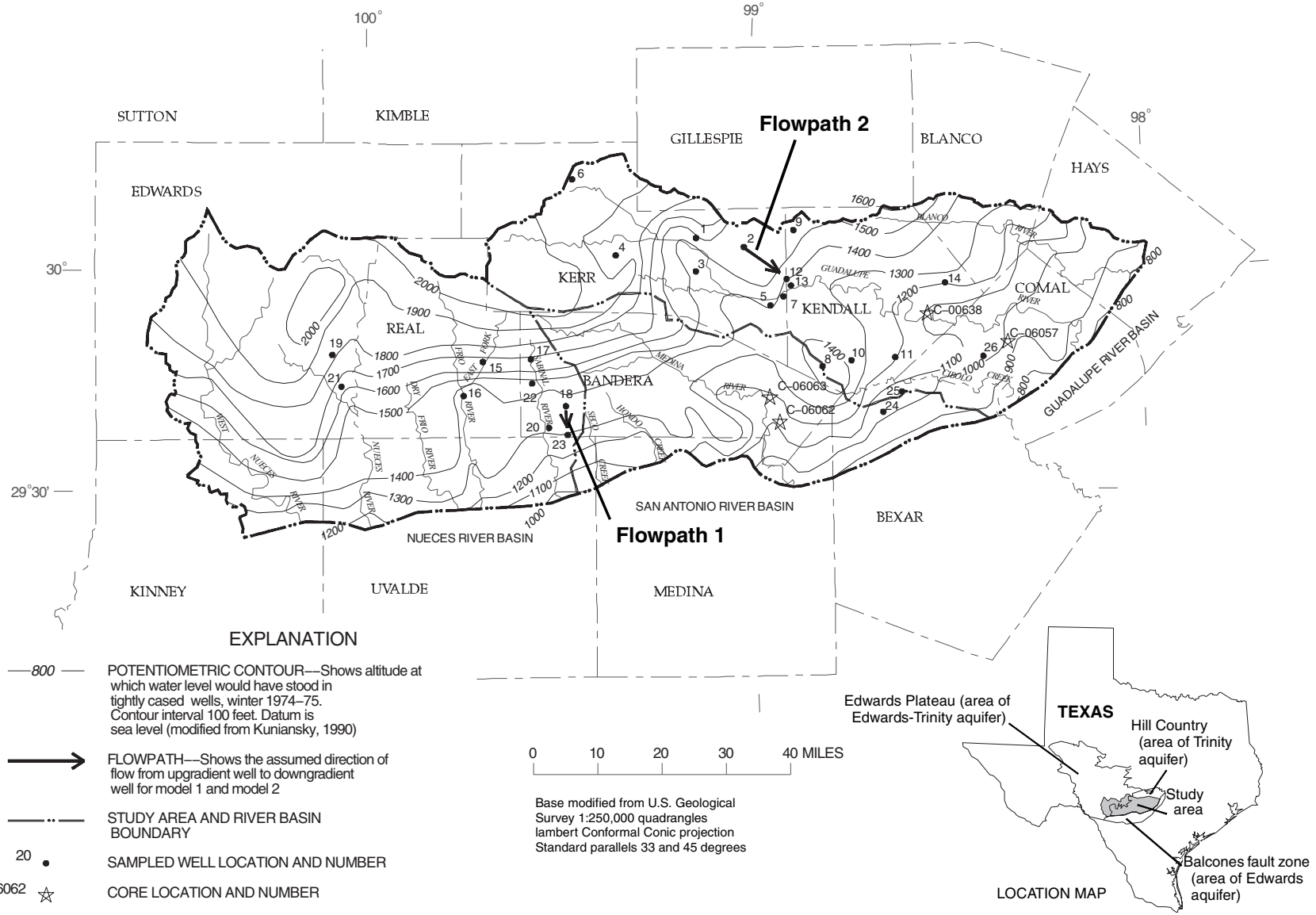

Figure 1. Potentiometric surface and locations of sampled wells and cores in the Trinity aquifer, south-central Texas.

STRATIGRAPHIC UNIT		HYDROGEOLOGIC UNIT	WATER-YIELDING PROPERTIES
Glen Rose Limestone	Upper member	Upper Trinity permeable zone	Yields <5 to 20 gallons per minute of fresh to moderately saline water.
Glen Rose Limestone	Lower member	Middle Trinity permeable zone	Yields 5 to 100 gallons per minute of fresh to slightly saline water.
Travis Peak equivalent	Hensel Sand		
Travis Peak equivalent	Cow Creek Limestone		
Travis Peak equivalent	Hammett Shale	Hammett confining unit	Considered a confining unit.
Travis Peak equivalent	Sligo Formation / Hosston Formation	Lower Trinity permeable zone	Yields 20 to >100 gallons per minute of fresh to slightly saline water

Figure 2. Relation among stratigraphic units, hydrogeologic units, and water-yielding properties of the Trinity aquifer, south-central Texas.

permeable zones (fig. 2) (Ashworth, 1983). Ashworth (1983) mapped the outcrop area of all three zones. The upper permeable zone of the Trinity aquifer consists of the upper member of the Glen Rose Limestone. The Glen Rose Limestone informally is subdivided into upper and lower members separated by a thin, widespread bed of fossilized *Corbula martinae*. The upper member has a maximum thickness of 450 feet (ft) and contains resistant and nonresistant beds of limestone and clay as well as two evaporite beds (Perkins, 1974). The alternating beds of limestone and calcareous clay erode differentially to produce the characteristic "stair-step" topography found in the Hill Country. Some of the resistant limestone beds are cut by streams and are above the regional potentiometric surface (Kuniansky, 1990).

The middle permeable zone of the Trinity aquifer is composed of the Cow Creek Limestone, Hensel Sand, and lower member of the Glen Rose Limestone. The Cow Creek Limestone is a massive, fossiliferous, fine- to coarse-grained calcarenite (Stricklin and Smith, 1973). The average thickness of the Cow Creek Limestone is 50 to 60 ft but can be as much as 90 ft. Updip, the Cow Creek Limestone thins to approximately 20 ft. Above the Cow Creek Limestone the updip continental deposits of the Hensel Sand are a poorly cemented mixture of clay, silt, sand, and conglomerates that grade into shaley marine deposits downdip. The thickness of the Hensel Sand varies from 80 to 300 ft and averages about 150 ft. The massive, fossiliferous lower member of the Glen Rose Limestone reaches a maximum thickness of about 320 ft.

The lower permeable zone of the Trinity aquifer is composed of the Hosston and Sligo Formations overlain by the Hammett Shale confining unit. The Hosston Formation consists of sandstone (largely composed of quartz sand derived from the Llano uplift area), mudstone, and claystone. The Sligo Formation is a sandy, dolomitic limestone downdip that represents the marine equivalent of the Hosston Formation. The sandstones and mudstones of the Hosston Formation and lower Sligo Formation are cemented by dolomite and contain dolomitic terrigenous detritus. The combined thicknesses of the Hosston and Sligo Formations are more than 500 ft in the downdip section of the study area. The Hammett Shale is a gray fossiliferous, calcareous,

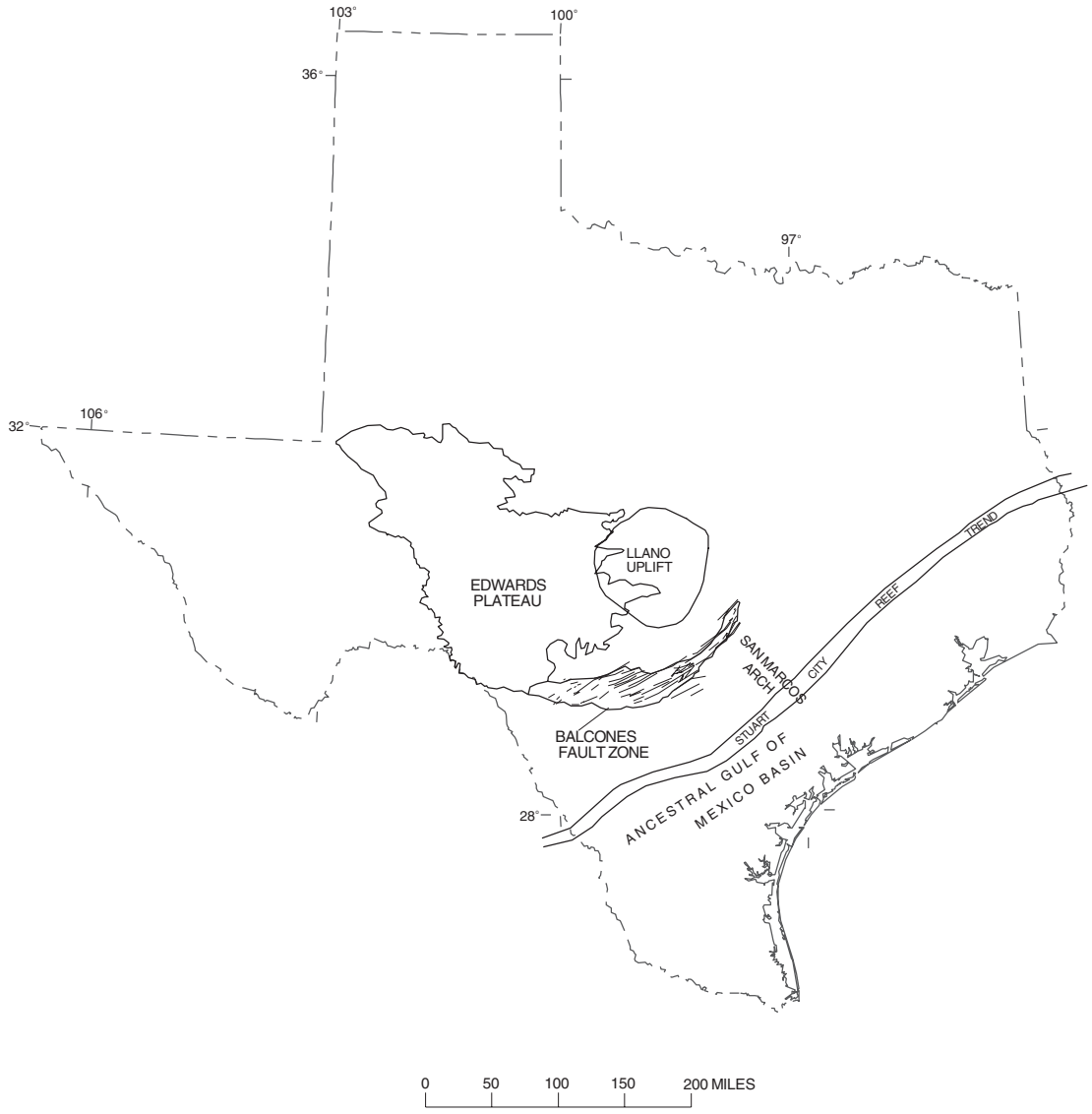

Figure 3. Structural and physiographic features associated with the Trinity aquifer of south-central Texas (modified from Barker and Ardis, 1996).

and dolomitic shale with thin interbeds of limestone and sand that pinch out in the updip parts of the study area. Downdip, the Hammett Shale is nearly 100 ft thick (Amsbury, 1974).

The Trinity aquifer is recharged by infiltration from losing streams, by infiltration of precipitation on outcrop areas, and by lateral inflow from the Edwards-Trinity aquifer to the northwest (Hammond, 1984; Kuniansky and Holligan, 1994). The upper permeable zone receives water directly from precipitation and leakage from streambeds. Because of the presence of soluble gypsum, most water in the upper permeable zone has greater dissolved solids concentrations than that in the middle permeable zone (Bush and others, 1994). The upper permeable zone discharges to springs and streams as well as to domestic and livestock wells. Recharge to the middle permeable zone occurs primarily by infiltration of precipitation where the units are exposed. Locally, vertical leakage from the overlying units also can contribute to recharge. Discharge from the middle permeable zone occurs by pumpage, by cross-formational flow to the Edwards aquifer to the southeast, and by springflow. The lower permeable zone receives recharge from the overlying middle permeable

zone where the Hammett Shale is missing, and from infiltration in the outcrop areas north of the study area. Discharge from the lower permeable zone occurs by wells and cross-formational flow to the Edwards aquifer.

Confined conditions dominate the regional ground-water system in the middle and lower permeable zones of the Trinity aquifer where the upper permeable zone has not been eroded. Locally, unconfined conditions exist near the surface. The altitude of the potentiometric surface in the aquifer (fig. 1) varies with the season and is directly affected by drought, above-average precipitation, and ground-water pumpage.

GEOCHEMISTRY OF THE TRINITY AQUIFER

Four rock cores from the middle permeable zone of the Trinity aquifer were analyzed to determine mineral content of the Trinity aquifer. Cores were selected for petrographic, X-ray fluorescence, X-ray diffraction, and isotopic analysis.

Ground-water samples were analyzed for field properties, major cations and anions, and isotopes. Water samples were not obtained from the upper permeable zone of the Trinity aquifer, and therefore, this zone is not discussed in the water-quality sections. Of the 26 water samples, 19 were collected from the middle permeable zone and 7 were collected from the lower permeable zone.

Data Compilation and Collection

Four cores from the middle permeable zone of the Trinity aquifer, 2 in Bandera County and 1 each in Comal and Kendall Counties (fig. 1), were selected for petrologic, mineralogic, bulk chemical, and isotopic analyses. The cores are stored at the repository of the Bureau of Economic Geology, University of Texas at Austin. Twenty-seven samples from the four cores were taken at 1-ft intervals, which resulted in 6 to 8 samples per core. X-ray diffraction analysis of these samples provided qualitative mineral identification using standard powder diffraction techniques (Hutchinson, 1974, p. 144–179). Petrographic analysis of thin sections provided a physical description of the rock fabric. X-ray fluorescence analysis (Taggart and others, 1987) provided bulk chemical analyses. Isotopic analyses provided carbon-13 ($\delta^{13}C$) data that were useful in constraining calculations of chemical mass transfer.

Suitable well sites for sampling were determined in a two-step process. First, broad areas of approximate directions of flow were drawn using the potentiometric-surface map of Kuniansky (1990) (fig. 1). Second, the records of the USGS and Texas Water Development Board were searched to locate wells completed in specific permeable zones within these areas. Well schedules were compiled, well owners contacted, and where possible, available wells inventoried. If a selected well was unavailable for sampling, an alternate well was selected from the available wells in the area. Except as noted, the water samples were collected according to the procedures outlined in Claassen (1982). Alkalinity and conductivity were measured in the field at the time of collection following the methods outlined in Wood (1976). The measurement of pH and temperature also followed the procedures of Wood (1976) with the exception that the measurements were made in a closed-system flow cell developed by the USGS Hydrologic Instrumentation Facility. Isotope samples were collected according to the procedures described in Busby and others (1991).

Petrology and Chemistry of Cores from the Trinity Aquifer

Although previous studies of the rocks composing the Trinity aquifer have described the geology of the area, limited petrologic, mineralogic, and chemical analyses were available. Three of the four cores selected for analyses for this investigation, C–06062, C–06063, and C–06057, were studied by Perkins (1974). Amsbury (1974) described core C–00638 and did petrological analyses on the lower section of the core, which includes rocks of the middle permeable zone.

The Glen Rose Limestone has been described extensively by several authors including Achauer (1977), who described reef outcrops from the Glen Rose Limestone in the Hill Country of Texas. Previous descriptions of outcrops are as shelf wackestones deposited in a subtidal to subaerial setting, consisting of low-magnesium calcite. A Glen Rose Limestone patch reef complex in Bandera County has been described as principally calcite, whereas nonreef areas consist of calcite and protodolomite. Fibrous cements present in the reef complex consist of low-strontium calcite. In dolomitic limestone, strontium concentrations range from 11 to 123 parts per million (ppm), sodium concentrations range from 0 to 3,987 ppm, and

chloride concentrations range from 0 to 3,390 ppm (Petta, 1977).

Hammond (1984) described the lower Glen Rose Limestone in Blanco, Kerr, Kendall, Comal, Bandera, Uvalde, Bexar, and Medina Counties. Hammond characterized the rocks as ledge-forming biomicrite and biosparite interbedded with a few thin layers of marl and marly biomicrite. The depositional sequence evolved in high energy, shallow marine, supratidal-to-tidal flats containing stromatolites and calcareous sands.

Results and descriptions from petrographic microscope analysis are given in table 1. Carbonate cements present are mostly micrite with some spar. Silica cement was observed in several cores but only in small quantities. In addition to the ions that can contribute to the aqueous phase, porosity is an important property that was addressed in the solid-phase analysis. Porosity varies from 2 to 64 percent with a mean of 15.6 percent. Ashworth (1983) measured porosities ranging from 1.0 to 37.5 percent, with a mean of 20 percent. Due to the heterogeneities in the Trinity aquifer, porosity varies considerably and can have a major effect on ground-water flow.

Core C–06062 is a recrystallized fossiliferous marine carbonate rock dominated by micrite cement. Porosity ranges from 5 to 24 percent with porosity of most samples between 10 and 14 percent.

Core C–06063 is carbonate rock consisting of micritic cement with zones of spar or calcite grains dominating the fabric. Siliceous cement is 1 percent or less, and porosity ranges from 4 to 30 percent throughout the core.

Core C–06057 is fossiliferous carbonate rock dominated by micritic cement with siliceous cement accounting for 1 percent or less; traces of dolomite were noted in the thin sections. Porosity ranges from 4 to 13 percent.

Core C–00638 primarily is fossiliferous carbonate rock dominated by micritic cement. Porosity in the upper 20 ft of the core ranges from 6 to 64 percent. The lower part varies from 2 to 23 percent porosity. Dolomicrite dominates the lower part of the core.

Results of X-ray fluorescence and X-ray diffraction analyses (table 2) are compatible with petrographic descriptions. Calcite dominates the cores, and dolomite and quartz are minor components. X-ray fluorescence showed calcium compositions reported as oxide near the 50- to 60-percent range in all cores. Magnesium composition reported as oxide varies from 0.49 to 3.81 percent. Silica is greatest in the upper intervals of cores C–06062, C–06063, and C–06057 and in the lower intervals of core C–00638. Total iron concentrations range from 500 to 10,000 ppm. Strontium concentrations range from 100 to 500 ppm.

Rock-core analyses provide information on minerals in solid phase present in the Trinity aquifer. On the basis of these four core analyses, calcite is the dominant mineral, but dolomite and quartz also are present. Other studies also indicate that gypsum and clay minerals are present in the middle Trinity aquifer (Stricklin and others, 1971; Perkins, 1974). The solid-phase minerals controlling water chemistry in the Trinity aquifer probably are calcite, dolomite, gypsum, and clay. These minerals include the following ions that could be added to the aqueous phase upon dissolution of the solid phase: calcium, magnesium, sulfate, sodium, and potassium. These ions are significant in the water chemistry of the Trinity aquifer.

Subsamples from four cores were selected for isotopic analysis of $\delta^{13}C$ and oxygen-18 ($\delta^{18}O$) (table 3). The $\delta^{13}C$ results are typical of marine carbonate rocks, which have a mean $\delta^{13}C$ value near 0 per mil (‰) and usually range from -4 to +4 ‰ (Hoefs, 1987). The $\delta^{18}0$ results appear to be in equilibrium with seawater, which usually ranges from -3 to 0 ‰.

Chemistry of Water in the Trinity Aquifer

Table 4 summarizes well data and results of laboratory analysis of water for field properties, cations, and anions from 26 wells in the Trinity aquifer of south-central Texas. The following sections describe these data.

Dissolved Solids

Dissolved solids concentrations in water from the 26 wells range from about 329 to about 3,030 milligrams per liter (mg/L). Of the water samples in this study, 6 had concentrations greater than 1,000 mg/L (3 samples from wells in the lower permeable zone and 3 samples from wells in the middle permeable zone). Among the sampled wells, dissolved solids concentrations generally increase from the northern boundary toward the interior of the study area. The southeastern part of the study area has the lowest dissolved solids concentrations in the study area.

Dissolved solids concentrations in 19 samples from the middle permeable zone range from 329 to 1,820 mg/L. Water from seven samples from the lower permeable zone had dissolved solids concentrations

Table 1. Results of petrographic microscope analyses of selected cores, middle permeable zone, Trinity aquifer, south-central Texas

[ft, feet; --, no data; mm, millimeter]

Core no. (fig. 1) and interval	Depth to bottom of sample (ft below land surface)	Percent cement			Percent grains	Percent porosity	Notes
		Micrite	Spar	Silica			
C–06062							
RL–101	120	52	6	--	28	14	Recrystallized calcite, dolomite, ferruginous, trace quartz
RL–102	166	70	15	--	2	13	Micrite cement, moldic porosity
RL–103	170	70	17	--	8	5	Micrite and microspar
RL–104	200	76	7	--	1	16	Peloidal grains, spar-filled molds
RL–105	203.3	56	18	--	2	24	Recrystallized peloids, large molds
RL–106	211	75	7	--	4	14	Micrite cement, moldic porosity to 5 mm
RL–107	220	82	3	--	5	10	Peloidal micrite, micropores
RL–108	230	36	37	trace	3	24	Large pores, cement, spar, some siliceous cement
C–06063							
RL–109	11.8	60	2	--	8	30	Macroporosity
RL–110	26	67	25	--	--	4	Recrystallized dolomicrite, no grains
RL–111	55.2	--	22	--	60	18	Peloids, porous, spar cement, algal grains
RL–112	73.3	16	40	--	18	26	Marine-cemented peloids, allochems
RL–113	90	4	46	--	35	15	Oolites and allochems with cement overgrowths, fracture-fill
RL–114	104	32	28	1	26	13	Peloids and oolites—fine-to-coarse spar, chert
C–06057							
RL–118	12.8	78	8	--	10	4	Dense micrite, peloidal, sparry, siliceous, microstylolites
RL–119	52.8	68	19	1	6	6	Micritic, microstylolites
RL–120	77.3	61	10	--	20	9	Dolomite rhombs, large oysters, diatoms and micrite, organic
RL–121	82.6	50	1	1	32	11	Siliceous rods with haloes, large vugs, chert, and micrite
RL–122	85.9	39	16	--	32	13	Clams and coral, quartz grains, porous, spar
RL–123	125	71	9	trace	8	12	Macropore, moldic, micrite matrix, spar
C–00638							
RL–124	6	30	6	--	--	64	Micrite
RL–125	16	63	16	--	2	19	Porous micritic peloidal grainstone
RL–126	20	53	39	trace	2	6	Sparry fill in molds, marine-cement, recrystallized peloids
RL–127	27	30	31	--	16	23	Marine-cemented peloids
RL–128	31.5	21	34	1	30	14	Micritized peloids, cemented, algal oolites, quartz grains
RL–129	33.5	66	22	--	10	2	Micritized grains, cemented, and replaced
RL–130	43	--	88	--	--	12	Dolomicrite, siliceous clasts, iron-stained

Table 2. Results of solid-phase analyses by X-ray fluorescence and X-ray diffraction of selected cores, middle permeable zone, Trinity aquifer, south-central Texas

[CaO, calcium oxide; MgO, magnesium oxide; Fe_2O_3, iron oxide; SiO_2, silica; Al_2O_3, aluminum oxide; K_2O, potassium oxide; Fe, iron; ppm, parts per million; Mn, manganese; Sr, strontium; Cr, chromium; Ti, titanium; V, vanadium. Diffraction: s, strong; --, no diffraction; m, moderate; w, weak; tr, trace; vw, very weak]

Core no. (fig. 1) and interval	X-ray fluorescence												X-ray diffraction		
	CaO (percent)	MgO (percent)	Fe_2O_3 (percent)	SiO_2 (percent)	Al_2O_3 (percent)	K_2O (percent)	Fe (ppm)	Mn (ppm)	Sr (ppm)	Cr (ppm)	Ti (ppm)	V (ppm)	Calcite	Dolomite	Quartz
C–06062															
RL–101	51.20	0.76	0.96	5.72	1.72	0.41	1,500	50	300	15	70	30	s	--	--
RL–102	56.3	.66	.08	.48	.15	.05	5,000	50	500	30	200	50	s	--	--
RL–103	53.00	2.31	.38	1.52	.41	.16	7,000	70	500	30	200	70	s	m	--
RL–104	56.60	.64	.04	.11	.10	.02	500	15	200	20	20	10	s	--	--
RL–105	56.50	.66	.04	.11	.10	.02	500	30	200	15	20	10	s	--	--
RL–106	55.80	.59	.04	.10	.10	.02	500	30	200	10	20	10	s	--	--
RL–107	57.00	.62	.04	.10	.10	.02	500	30	200	10	20	10	s	--	--
RL–108	57.20	.61	.04	.10	.10	.02	500	30	200	10	20	10	s	--	--
C–06063															
RL–109	55.90	.55	.08	1.10	.18	.05	1,500	30	300	10	50	15	s	--	--
RL–110	52.70	.84	.46	4.04	1.30	.34	5,000	50	100	20	500	30	s	--	w
RL–111	55.50	.51	.04	1.02	.13	.04	700	30	300	15	70	10	s	--	w
RL–112	56.30	.50	.04	.13	.10	.02	500	20	300	10	20	10	s	--	--
RL–113	56.20	.56	.04	.50	.10	.03	500	30	300	15	20	20	s	--	--
RL–114	56.10	.63	.12	.84	.17	.06	3,000	30	300	30	50	15	s	--	--
C–06057															
RL–118	51.90	.74	.47	5.17	1.19	.31	5,000	150	300	30	300	70	s	--	--
RL–119	54.40	.78	.15	1.64	.46	.14	2,000	30	500	15	150	30	s	--	--
RL–120	53.40	1.43	1.18	1.15	.27	.09	10,000	30	300	15	150	10	s	w	tr
RL–121	56.30	.80	.07	.34	.10	.03	1,500	30	500	15	20	15	s	vw	--
RL–122	55.40	.87	.08	.73	.12	.05	700	30	500	10	20	15	s	--	--
RL–123	52.70	1.12	.65	3.25	.63	.18	7,000	70	500	20	300	30	s	--	--
C–00638															
RL–124	55.90	.82	.10	.73	.10	.05	700	50	300	10	20	20	s	tr	tr
RL–125	55.30	1.20	.04	.64	.16	.05	500	50	300	10	30	30	s	tr	tr
RL–126	56.20	.62	.04	.62	.18	.06	500	50	300	10	20	30	s	w	tr
RL–127	56.70	.49	.04	.61	.10	.03	500	50	300	10	20	10	s	vw	--
RL–128	55.80	.59	.08	1.51	.14	.07	700	30	150	10	20	15	s	--	--
RL–129	53.50	.69	.29	4.44	.46	.16	2,000	150	200	10	200	20	s	--	--
RL–130	47.80	3.81	.60	6.67	.61	.25	7,000	200	500	30	300	30	s	m	w

Table 3. Results of isotopic analyses of selected cores, middle permeable zone, Trinity aquifer, south-central Texas

[‰, per mil]

Core no. (fig. 1) and interval	$\delta^{13}C$ (‰)	$\delta^{18}O$ (‰)
C–06062		
RL–103	+3.7	-2.5
RL–107	+3.4	-4.1
C–06063		
RL–110	-4.0	-2.6
RL–113	+2.6	-3.4
C–06057		
RL–118	+2.1	-2.3
RL–120	+4.5	-1.8
C–00638		
RL–129	+1.6	-2.8
RL–130	-3.7	-2.6

ranging from 518 to 3,030 mg/L. Generally, the water from the lower permeable zone has a greater dissolved solids concentration than from the middle permeable zone. Water from wells 1 and 2, which have dissolved solids concentrations of 518 mg/L and 651 mg/L, respectively, have lower concentrations than the other wells sampled in the lower permeable zone. Bush and others (1994) report a median dissolved solids concentration of 510 mg/L for the middle permeable zone of the Trinity aquifer and 652 mg/L for the lower permeable zone on the basis of 224 and 71 analyses, respectively.

Major Ions

Dissolved calcium concentrations range from 1.3 to 5.7 millimoles per liter (mmol/L[1]) in the middle permeable zone and 0.77 to 9.7 mmol/L in the lower permeable zone (table 4). Dissolved magnesium concentrations range from 0.86 to 8.2 mmol/L in the middle permeable zone and from 0.82 to 10.3 mmol/L in the lower permeable zone. Because dissolution of dolomite releases 1 mole of magnesium for every mole of calcium released, and molar ratios of calcium/magnesium approach or are approximately 1 (fig. 4) in the western and northern parts of the study area, waters are probably in contact with rocks containing dolomite.

Calcium and magnesium concentrations increase as the concentration of sulfate increases (fig. 4). The exception to this trend is in the extreme southeastern part of the study area near Cibolo Creek, where concentrations of calcium ions are greater than concentrations of magnesium ions in water from wells 10, 11, 24, 25, and 26 (fig. 1). This area probably is an area of recharge for the Trinity aquifer (P.W. Bush, U.S. Geological Survey, oral commun., 1993). Dissolution of calcite is likely the dominant geochemical process.

Dissolved sodium concentrations vary from 0.33 to 4.8 mmol/L in the middle permeable zone and from 0.70 to 18.3 mmol/L in the lower permeable zone. Dissolved sodium concentrations generally are greater in the lower permeable zone than the middle permeable zone. This difference could be caused by a longer residence time of ground water in the lower permeable zone. Dissolved chloride concentrations range from 0.26 to 5.4 mmol/L in the middle permeable zone and from 0.96 to 11.6 mmol/L in the lower permeable zone. The dissolved chloride concentration in water from well 12, lower permeable zone, is 11.6 mmol/L, almost double the concentration in water from well 19 and greater than any other sample from wells in the study area. The sodium-to-chloride mole ratios are greater than 1, indicating a source for the excess sodium other than halite or fluid inclusions containing seawater. Cation

[1]Major ions reported in millimoles per liter rather than in milligrams per liter to be consistent with mass-transfer discussions and calculations.

Table 4. Summary of well data and results of chemical analyses of ground-water samples, Trinity aquifer, south-central Texas

[Depths in feet below land surface. ft, feet; °C, degrees Celsius; mmol/L, millimoles per liter; mg/L, milligrams per liter; --, no data]

Well no. (fig. 1)	Station ID	County	Permeable zone	Depth to top of permeable zone sampled (ft)	Depth of well, total (ft)	Altitude of land surface (ft above sea level)	pH[1] (standard units)	Temperature[1] (°C)	Calcium, dissolved (mmol/L)	Magnesium, dissolved (mmol/L)	Sodium, dissolved (mmol/L)	Potassium, dissolved (mmol/L)	Bicarbonate[1] (mmol/L)	Sulfate, dissolved (mmol/L)	Chloride, dissolved (mmol/L)	Dissolved solids (mg/L)
1	300424099090001	Kerr	Lower	--	725	1,700	7.20	22.7	1.5	1.8	0.70	0.14	6.4	0.26	0.96	518
2	300307099013701	Kerr	Lower	369	690	1,900	7.10	22.6	2.3	2.1	2.2	.25	5.7	2.0	2.0	651
3	295954099090401	Kerr	Middle	275	600	1,780	7.10	22.6	3.5	3.2	1.0	.26	5.9	4.5	.48	892
4	300209099212601	Kerr	Middle	200	437	1,800	7.25	21.6	3.2	3.5	1.2	.36	5.0	5.1	.56	929
5	295513098573601	Kerr	Middle	235	485	1,640	7.19	22.7	1.7	2.0	1.1	.28	6.4	1.3	.59	504
6	301223099280701	Kerr	Middle	515	600	2,158	7.15	22.3	1.3	1.7	.87	.21	6.0	.52	.34	380
7	295625098553401	Kerr	Middle	178	441	1,541	7.22	23.9	2.1	2.1	2.0	.33	6.0	1.6	1.9	603
8	294659098494001	Kendall	Middle	436	600	1,700	7.07	21.6	1.7	2.3	3.9	.38	5.4	2.5	2.1	721
9	300519098535501	Kendall	Middle	355	550	1,880	7.07	21.6	1.6	1.7	2.3	.23	5.4	.58	2.4	481
10	294744098451201	Kendall	Middle	60	152	1,510	6.89	21.0	5.7	2.8	.52	.06	5.4	5.7	.59	1,060
11	294805098382701	Kendall	Middle	200	346	1,400	6.90	21.0	3.2	1.0	4.8	.17	7.2	.61	5.4	776
12	295846098550201	Kendall	Lower	--	--	1,487	7.12	23.4	2.7	2.5	9.6	.43	5.7	2.0	11.6	1,200
13	295753098542301	Kendall	Middle	--	--	1,418	7.01	22.0	2.2	2.2	3.6	.31	6.5	1.6	4.5	759
14	295800098303401	Kendall	Middle	95	180	1,350	7.10	21.4	2.2	.99	.33	.03	6.7	.12	.37	365
15	294755099420301	Real	Lower	677	1,000	1,752	7.50	28.4	.90	.99	8.7	.31	6.2	1.8	3.1	756
16	294322099450101	Real	Lower	605	940	1,580	7.48	28.2	.77	.82	10.0	.33	6.4	1.7	3.7	792
17	294815099343801	Bandera	Middle	300	770	1,824	7.22	26.0	2.3	2.7	2.4	.46	5.4	3.3	.96	767
18	294157099291601	Bandera	Middle	65	505	1,647	7.14	22.8	4.2	4.0	.70	.17	5.2	5.7	.28	1,020
19	294854100051501	Edwards	Lower	26	936	1,800	7.32	28.2	1.8	2.1	18.3	.61	6.3	7.0	6.2	1,670
20	293903099315401	Bandera	Middle	60	440	1,421	7.31	23.7	1.6	2.0	.52	.08	5.1	1.2	.26	413
21	294438100035001	Edwards	Lower	450	735	1,660	7.00	26.5	9.7	10.3	6.5	.97	4.7	20.8	1.2	3,030
22	294500099342701	Bandera	Middle	500	873	1,680	7.17	25.4	3.0	3.4	2.8	.51	5.3	5.1	.99	989
23	293805099290101	Bandera	Middle	150	440	1,418	6.99	24.3	5.5	8.2	2.5	.56	5.9	11.4	.73	1,820
24	294046098402501	Bexar	Middle	290	505	1,371	7.20	22.0	2.2	.86	.40	.03	5.9	.14	.42	343
25	294377098372701	Bexar	Middle	300	525	1,314	7.25	22.5	1.8	1.2	.48	.06	5.3	.24	.54	329
26	294803098245101	Comal	Middle	400	500	1,245	7.07	23.3	2.5	.95	.48	.06	6.4	.17	.48	380

[1] Measured at well site.

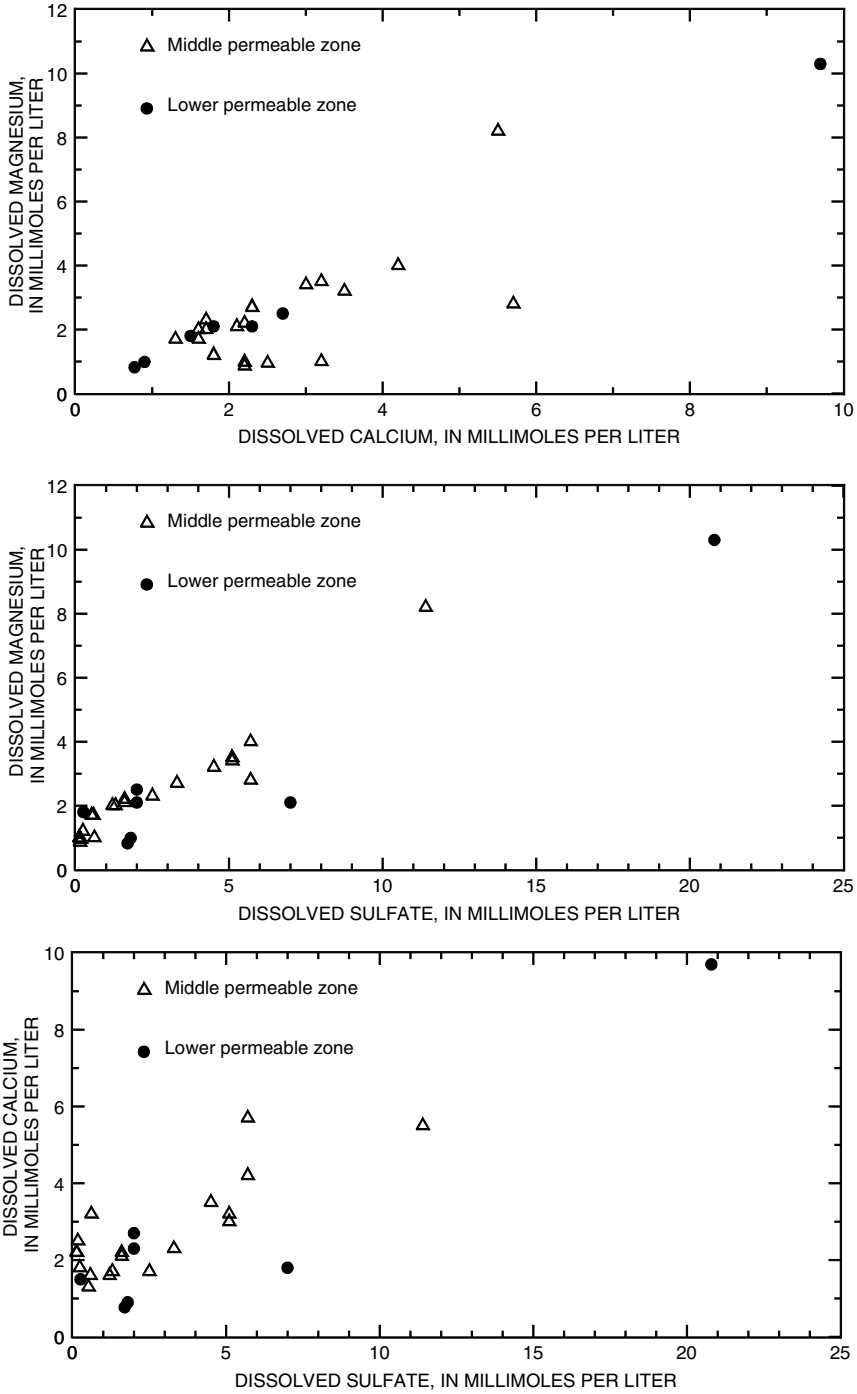

Figure 4. Relation of dissolved magnesium to dissolved calcium, dissolved magnesium to dissolved sulfate, and dissolved calcium to dissolved sulfate for samples collected from the Trinity aquifer, south-central Texas.

exchange of calcium and (or) magnesium for sodium in clays is a possible alternative source. When sodium concentrations are greater than chloride concentrations, the exchange of calcium ions and magnesium ions in solution for sodium ions on clays could account for the excess sodium. When chloride concentrations are greater than sodium concentrations, a reverse exchange might be occurring. These statements hold true if sodium chloride dissolution and cation exchange are the principal sources of sodium and chloride ions.

Dissolved potassium concentrations range from 0.03 to 0.56 mmol/L in the middle permeable zone and from 0.14 to 0.97 mmol/L in the lower permeable zone. The largest concentrations occur in the western part of the study area. Dissolved potassium concentrations in the middle permeable zone are lower than in the lower permeable zone with 12 of 19 samples having dissolved potassium concentrations of less than 0.30 mmol/L. Five of the seven wells in the lower permeable zone have dissolved potassium concentrations greater than 0.30 mmol/L. The lowest concentrations are in the southeastern part of the study area where recharge water probably is affecting water chemistry. Dissolved sulfate concentrations range from 0.12 to 11.4 mmol/L in the middle permeable zone and from 0.26 to 20.8 mmol/L in the lower permeable zone.

pH and Bicarbonate Alkalinity

pH and alkalinity are affected principally by rock-water interactions in the aquifer. As calcite precipitates, pH decreases with a resulting increase in the partial pressure of carbon dioxide (P_{CO_2}) (fig. 5). Alkalinity is a measure of inorganic carbon in ground water. Alkalinity as bicarbonate principally is produced from carbonate reactions with aqueous carbon dioxide derived from the atmosphere and from soil carbon dioxide entering the aquifer in recharge areas. Additional bicarbonate could be derived from oxidation of organic matter (eq. 1).

oxidation of organic matter

$$CH_2O + O_2 \longrightarrow HCO_3^- + H^+. \qquad (1)$$

Most of the middle permeable zone and all of the lower permeable zone are assumed to be closed systems in the study area, that is, no atmospheric or soil-generated carbon dioxide enters the systems after recharge, except in the southeastern part of the study area.

pH ranges from 6.89 to 7.31 in the middle permeable zone and from 7.00 to 7.50 in the lower permeable zone. Bicarbonate alkalinity ranges from 5.0 to 7.2 mmol/L in the middle permeable zone and from 4.7 to 6.4 mmol/L in the lower permeable zone.

Environmental Isotopes

Selected environmental isotopes are useful in ground-water studies (Fritz and Fontes, 1980). Thorough discussions of uses and reporting units for environmental isotopes are given in Fritz and Fontes (1980). Tritium, the radioactive isotope of hydrogen (^3H), is used to distinguish between water that entered an aquifer prior to thermonuclear testing and water that was introduced to the aquifer after thermonuclear testing began (Domenico and Schwartz, 1990). $\delta^{13}C$ is most useful for identifying sources of carbon, such as organic matter ($\delta^{13}C$ relatively negative) and carbonate minerals ($\delta^{13}C$ relatively positive). Analyses of $\delta^{18}O$ and deuterium (δD) can be used to determine possible sources (meteoric or brine) of water contributing to an aquifer. Sulfur-34 ($\delta^{34}S$) is used most widely to distinguish different sources of sulfur in ground water. ^{14}C typically is used to determine the time since water was last in contact with the atmosphere (Drever, 1988).

All tritium concentrations in samples from wells in the study area are less than 6 tritium units (TU) (table 5). Water from wells 10, 11, 13, 24, and 26 in the eastern part of the study area contain measurable amounts of tritium. In the western part of the study area, water from well 18 contains 1.2 TU. Water sampled from the lower permeable zone does not have detectable amounts of tritium.

$\delta^{13}C$ ranges from -10.7 to -1.6 ‰ in the study area, with water from most wells ranging from -9.0 to -6.6 ‰. This range is consistent with dissolution and precipitation of carbonates in a marine limestone aquifer, with some contribution from soil weathering (Anderson and Arthur, 1983; and Hoefs, 1987). $\delta^{13}C$ ranges from -10.7 to -1.6 ‰ in the middle permeable zone and from -10.0 to -2.1 ‰ in the lower permeable zone. In the western part of the study area, $\delta^{13}C$ ranges from -7.0 to -1.6 ‰. Values of $\delta^{13}C$ are lighter (more negative) in samples from the northernmost part of the study area and are heavier (more positive) than -2.0 ‰ in samples from near the southern part of the study area.

δD and $\delta^{18}O$ data obtained from global precipitation surveys correlate according to the linear relation (Dansgaard, 1964)

$$\delta D = 8\ \delta^{18}O + 10, \qquad (2)$$

which is the meteoric water line. In the middle permeable zone, $\delta^{18}O$ ranges from -5.4 to -4.2 ‰ and δD ranges from -32.4 to -22.5 ‰. In the lower permeable zone, $\delta^{18}O$ ranges from -5.3 to -4.9 ‰ and δD ranges from -31.0 to -29.0 ‰. These values are reasonably consistent with the meteoric water line (fig. 6), which indicates the origin of the water in the Trinity aquifer is from precipitation.

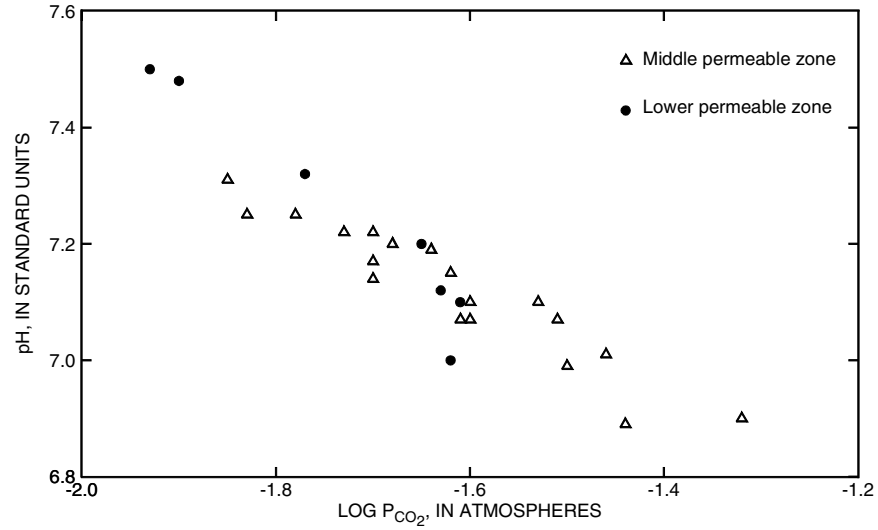

Figure 5. Relation of pH to partial pressure of carbon dioxide (P_{CO_2}) for samples collected from the Trinity aquifer, south-central Texas.

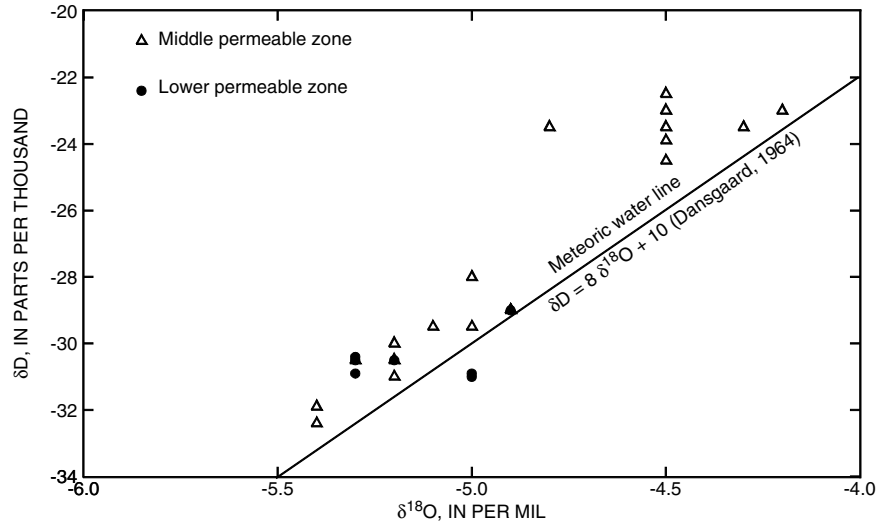

Figure 6. Relation of deuterium (δD) to oxygen-18 ($\delta^{18}O$) for samples collected from the Trinity aquifer, south-central Texas.

$\delta^{34}S$ ranges from -9.4 to 20.2 ‰ in the middle permeable zone and from 10.5 to 22.8 ‰ in the 1ower permeable zone. With the exception of water from wells 11 and 14 (middle permeable zone), $\delta^{34}S$ is relatively heavy, ranging from 9.1 to 22.8 ‰. Water from wells 11 and 14, with $\delta^{34}S$ of 0.6 and -9.4 ‰, respectively, could reflect sources of sulfate lighter in $\delta^{34}S$, such as pyrite oxidation, near recharge areas. The heaviest values are in water from wells in the western part of the study area. Nearly all of the $\delta^{34}S$ isotopic content could come from sulfate dissolved from trace amounts of gypsum present in the Trinity aquifer. Because all samples of ground water are undersaturated with respect to gypsum and samples contain no sulfide (indicating no sulfate reduction), sulfate is assumed to be conservative.

^{14}C varies across the study area ranging from 0.3 to 68.6 percent modern carbon (pmc) in water from the middle permeable zone and from 0 to 1.6 pmc in water from the lower permeable zone. In the eastern part of the study area near Cibolo Creek, ^{14}C values are 68.6

Table 5. Results of isotopic analyses of ground-water samples and calculated WATEQF saturation indices for selected minerals and partial pressure of carbon dioxide (P_{CO_2}), Trinity aquifer, south-central Texas

[TU, tritium units; ‰, per mil; pmc, percent modern carbon; <, less than; --, no data]

Well no. (fig. 1)	Permeable zone	Tritium (TU)	$\delta^{13}C$ (‰)	$\delta^{18}O$ (‰)	δD (‰)	$\delta^{34}S$ (‰)	^{14}C (pmc)	Saturation index			Log P_{CO_2} (atmospheres)
								Calcite	Dolomite	Gypsum	
1	Lower	<0.8	-10.0	-5.0	-31.0	10.5	<0.1	0.02	0.23	-2.34	-1.65
2	Lower	<.8	-7.8	-5.0	-30.9	14.4	1.6	.00	.05	-1.36	-1.61
3	Middle	<.8	-7.5	-5.4	-31.9	11.9	<.1	.12	.29	-.93	-1.60
4	Middle	<.8	-6.6	-5.2	-30.5	--	<.5	.14	.39	-.92	-1.83
5	Middle	<.8	-7.0	-5.0	-29.5	13.5	<.5	.05	.26	-1.64	-1.64
6	Middle	<.8	-7.7	-5.4	-32.4	9.1	<.8	-.12	-.02	-2.08	-1.62
7	Middle	<.8	-7.4	-4.9	-29.0	14.0	<.5	.12	.36	-1.50	-1.70
8	Middle	<.8	-1.6	-5.1	-29.5	--	<.5	-.22	-.22	-1.40	-1.61
9	Middle	<.8	-8.1	-5.2	-30.0	10.0	<.5	-.19	-.26	-1.98	-1.60
10	Middle	5.3	-7.8	-4.5	-23.9	16.1	--	.05	-.13	-.67	-1.44
11	Middle	5.3	-10.7	-4.5	-23.5	.6	--	.04	-.34	-1.71	-1.32
12	Lower	<.8	-7.7	-4.9	-29.0	19.5	<.4	.06	.18	-1.37	-1.63
13	Middle	2.6	-9.0	-4.9	-29.0	13.3	--	-.06	-.04	-1.49	-1.46
14	Middle	<.8	-6.8	-4.3	-23.5	-9.4	--	.10	-.04	-2.47	-1.53
15	Lower	<.8	-6.0	-5.3	-30.5	16.5	<.4	.10	.41	-1.78	-1.93
16	Lower	<.8	-6.5	-5.2	-30.5	--	.6	.03	.24	-1.86	-1.90
17	Middle	<.8	-5.7	-5.3	-30.5	17.4	<.4	.11	.41	-1.19	-1.73
18	Middle	1.2	-4.5	-4.8	-23.5	20.2	18.4	.17	.40	-.79	-1.70
19	Lower	<.8	-7.0	-5.3	-30.9	22.8	<.4	.06	.33	-1.12	-1.77
20	Middle	<.8	-1.8	-4.2	-23.0	16.5	8.3	.07	.34	-1.68	-1.85
21	Lower	<.8	-2.1	-5.3	-30.4	18.6	.7	.18	.51	-.20	-1.62
22	Middle	<.8	-1.9	-5.2	-31.0	17.5	.3	.10	.38	-.96	-1.70
23	Middle	<.8	-1.6	-5.0	-28.0	19.8	1.2	.10	.48	-.55	-1.50
24	Middle	4.7	-8.0	-4.5	-23.0	--	68.6	.17	.03	-2.41	-1.68
25	Middle	<.8	-3.2	-4.5	-24.5	--	23.4	.10	.10	-2.25	-1.78
26	Middle	5.3	-7.0	-4.5	-22.5	--	61.9	.14	-.03	-2.30	-1.51

and 61.9 pmc in wells 24 and 26 (middle permeable zone), respectively, indicating the youngest water sampled in the study area. In the central part of the study area, near the Sabinal River, ^{14}C values of 18.4 and 8.3 pmc were computed for water from wells 18 and 20 (middle permeable zone). The ^{14}C values for water from wells 18 and 20 represent the youngest water sampled in the central part of the study area.

CHEMICAL EVOLUTION OF WATER IN THE TRINITY AQUIFER

The mass-transfer model NETPATH (Plummer and others, 1991) was used to calculate the net amount of dissolution and precipitation of selected minerals along an assumed flowpath between upgradient and downgradient wells, which is necessary to calculate travel time of water between wells. The ground-water flowpaths used for this report were selected to be consistent with the regional direction of ground-water flow as determined by the 1974–75 potentiometric-surface map of Kuniansky (1990). A 1988–90 potentiometric-surface map shows a similar pattern of regional potentiometric-contour lines (K.H. Wynn, U.S. Geological Survey, written commun., 1992). Although the 1974–75 potentiometric surface combines the three permeable zones of the Trinity aquifer, it is assumed that flow in each permeable zone is in approximately the same direction. Potentiometric-surface maps of the individual permeable zones (Ashworth, 1983) support the use of the combined-zone potentiometric surface for selection of flowpaths. Two approximate flowpaths (fig. 1) were chosen for application of the mass-transfer model NETPATH. Flowpath 1, in the middle permeable zone, is from upgradient well 18 to downgradient well 23. Flowpath 2, in the lower permeable zone, is from upgradient well 2 to downgradient well 12. From the set of wells sampled in the study area for this investigation, these wells provided the only acceptable flowpaths on the basis of chemical and isotopic data.

Hydrochemical Facies and Evolution

Hydrochemical facies were determined on the basis of analyses of water from sampled wells and use of the trilinear diagram (fig. 7). Hydrochemical facies of the middle permeable zone generally are calcium magnesium bicarbonate and calcium magnesium sulfate. Calcium bicarbonate facies occur primarily in the eastern part of the study area. In the western part, a combination of calcium sulfate and sodium sulfate predominate. The hydrochemical facies in the lower permeable zone vary. Sodium mixed-anion facies are predominant in wells 15 and 16. Wells 19 and 21 produce ground water that contains large quantities of sulfate.

The trilinear diagram of water from the middle permeable zone indicates a dedolomitization pattern (Hanshaw and Back, 1979) along several flowpaths; that is, a recharge water of calcium magnesium bicarbonate facies changes downgradient to a water of magnesium calcium sulfate facies. Dedolomitization is the process by which dolomite dissolution occurs (eq. 3) as gypsum dissolves (eq. 4) and calcite precipitates (eq. 5):

$$\text{dolomite dissolution} \quad CaMg(CO_3)_2 + 2H_2O + 2CO_2 \rightarrow Ca^{2+} + Mg^{2+} + 4HCO_3^-, \tag{3}$$

$$\text{gypsum dissolution} \quad CaSO_4 \bullet 2H_2O \rightarrow Ca^{2+} + SO_4^{2-} + 2H_2O, \tag{4}$$

$$\text{calcite precipitation} \quad Ca^{2+} + 2HCO_3^- \rightarrow CaCO_3 + CO_2 + H_2O. \tag{5}$$

The resulting pattern on the trilinear diagram is ground water, initially a calcium magnesium bicarbonate facies, which evolves toward a magnesium calcium sulfate facies along a ground-water flowpath. Water from wells 14, 24, 25, and 26 yield water with constituent concentrations representative of recharge; that is, a calcium magnesium bicarbonate facies. Wells 3, 4, 10, 18, and 23 yield water with constituent concentrations more representative of downgradient (magnesium calcium sulfate facies) conditions.

The chemical data describing lower permeable zone facies were too variable to characterize hydrochemical facies evolution. Sodium chloride dissolution, cation exchange, and dedolomitization are all plausible processes in the lower permeable zone (fig. 7).

Rock-Water Interaction Modeling

As a first step in the modeling of rock-water interactions, a modified version of the aqueous speciation code WATEQF (Plummer and others, 1976) was used with analytical data to determine the saturation indices (SI) of minerals present in the Trinity aquifer. The saturation state for a mineral or other participating substance is expressed as SI,

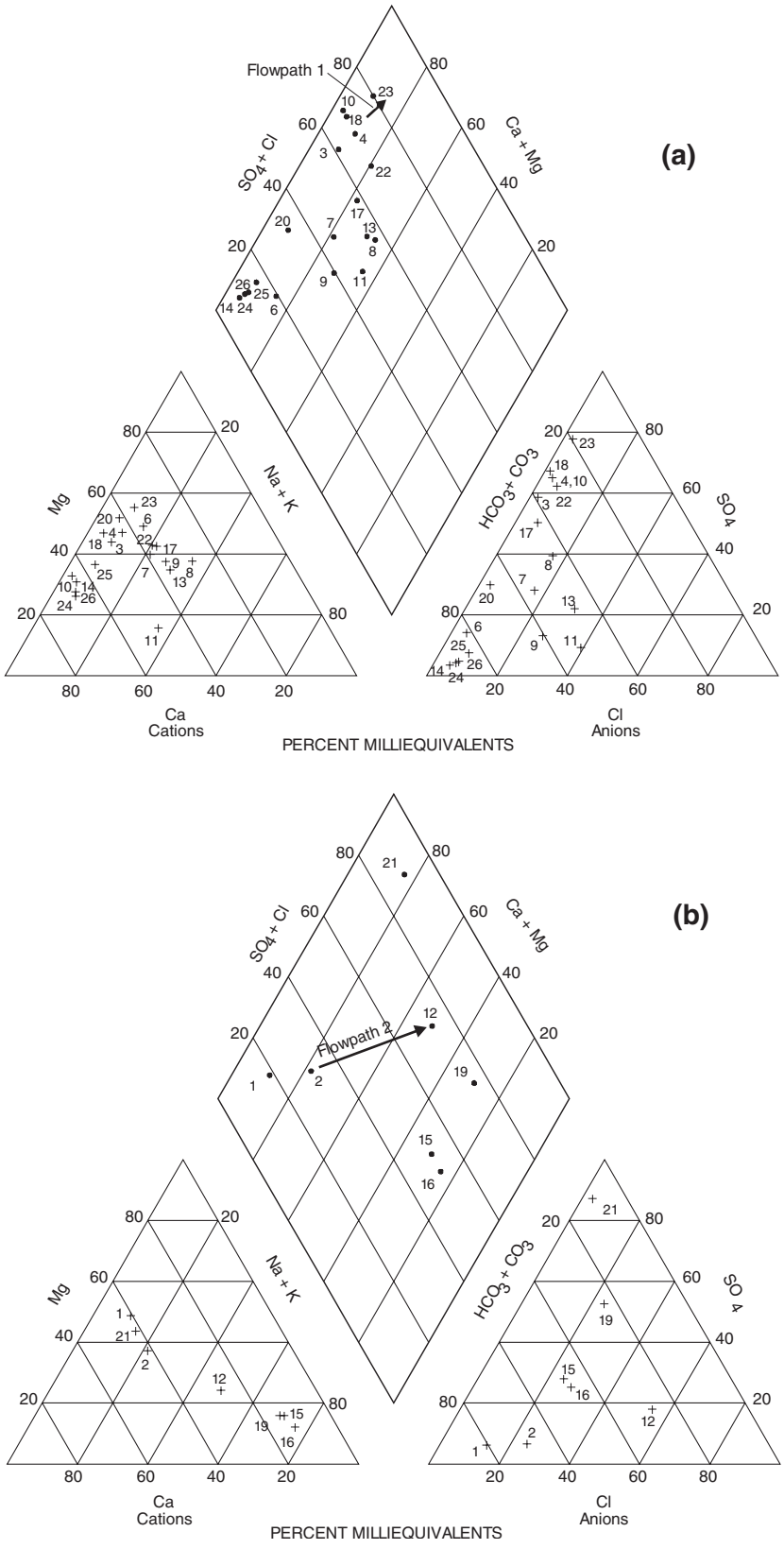

Figure 7. Trilinear diagrams of waters from the (a) middle and (b) lower permeable zones of the Trinity aquifer, south-central Texas. (Arrows indicate selected flowpaths.)

$$SI = \log_{10} IAP/K, \quad (6)$$

where

SI is saturation index;

IAP is ionic activity product; and

K is mineral equilibrium constant at a specified temperature.

In general, when SI is positive, the specific mineral is oversaturated and precipitation is possible; when SI is zero, the specific mineral is saturated and precipitation or dissolution is possible; when SI is negative, the specific mineral is undersaturated and dissolution is possible. Accuracy of calculated SI is variable because of differences in mineral stoichiometries, analytical accuracy, errors in pH (caused in part by outgassing of CO_2 during sample collection), and errors in thermodynamic data. In general, a range of accuracy of ±0.1 for calcite and gypsum and ±0.2 for dolomite is expected.

The SIs for calcite, dolomite, and gypsum are shown in table 5, and each is graphed as a function of dissolved sulfate concentration (fig. 8). Calcite was near saturation in all water sampled (table 5). SI for dolomite varied, but all water sampled was within ±0.5 of saturation except water from well 21, which had an SI of 0.51. The negative SIs for gypsum indicate undersaturation; and the relatively smooth trend toward saturation as the sulfate concentration increases (fig. 8) does not indicate significant amounts of sulfate reduction. Because gypsum dissolves during dedolomitization, sulfate concentration can be considered as an indication of reaction progress. The SIs for selected minerals, determined by WATEQF, were compared to the predicted mass-transfer results of NETPATH for consistency. For example, if results from NETPATH (next section) indicated a mineral was dissolving, then WATEQF also should indicate the mineral was undersaturated or near saturation.

Mass-Transfer Modeling

The second step in the modeling process was to use NETPATH to determine mass transfer between the solid and aqueous phase that occurs as water flows downgradient. Field measurements of pH, temperature, and alkalinity (table 4); concentrations of dissolved chemical constituents (table 4); thermodynamic data from WATEQF (table 5); and $\delta^{13}C$ and ^{14}C (table 5) were used as input for the mass-transfer model. $\delta^{13}C$ values for the solid-phase modeling are derived from unpublished core data or published values for a marine limestone (Hoefs, 1987). $\delta^{34}S$ values for the solid-phase modeling are from published values for oceanic sulfate (Hoefs, 1987).

NETPATH modeling parameters

Flowpath	$\delta^{34}S$ (‰)[1]	Ion exchange (XMg)[2]	Proportion of CO_2 in gas[3]	$\delta^{13}C$ (‰)	
				Organic matter	Carbonate minerals
1	22.0	0.0	1.0	-25.0	1.6
2	22.0	0.0	1.0	-25.0	0.0

[1] Dissolving gypsum.

[2] XMg is the fraction of magnesium/sodium ion exchange; 0.0 = pure calcium/sodium ion exchange; 1.0 = pure magnesium/sodium ion exchange.

[3] Proportion of carbon dioxide gas in a carbon dioxide-methane mixture; 0.0 = pure methane gas; 1.0 = pure carbon dioxide gas.

Results of mass-transfer simulation along flowpath 1 (table 6) for the middle permeable zone show dolomite, gypsum, and a small amount of sodium chloride dissolved. Calcite was precipitated, and a small amount of dissolved calcium was exchanged for sodium. The small CO_2 loss could have been from degassing of the sample during collection or the possibility of a partially open system along the flowpath. Dissolution of dolomite is driven by dissolution of gypsum with precipitation of calcite, and production of CO_2 gas. An overall pH decrease resulting from the geochemical process of dedolomitization was simulated along flowpath 1.

Results of mass-transfer simulation along flowpath 2 (table 6) for the lower permeable zone show smaller amounts of dolomite and gypsum dissolved and a large amount of sodium chloride dissolved. Calcite is shown to precipitate. Some reverse cation exchange (sodium for calcium) between solid and aqueous phases was indicated. This reverse cation exchange could result from excess sodium in the model, which might be caused by an analytical error in one of the chemical analyses.

FLOW VELOCITY ESTIMATES

The mass transfers calculated using NETPATH were used to adjust the initial ^{14}C concentration (in pmc) measured at each upgradient well by considering all sources and sinks of carbon which affect the carbon mass transfer between initial and final wells along the assumed flowpaths 1 and 2. Radioactive decay of ^{14}C occurs with a half-life of 5,730 years. However,

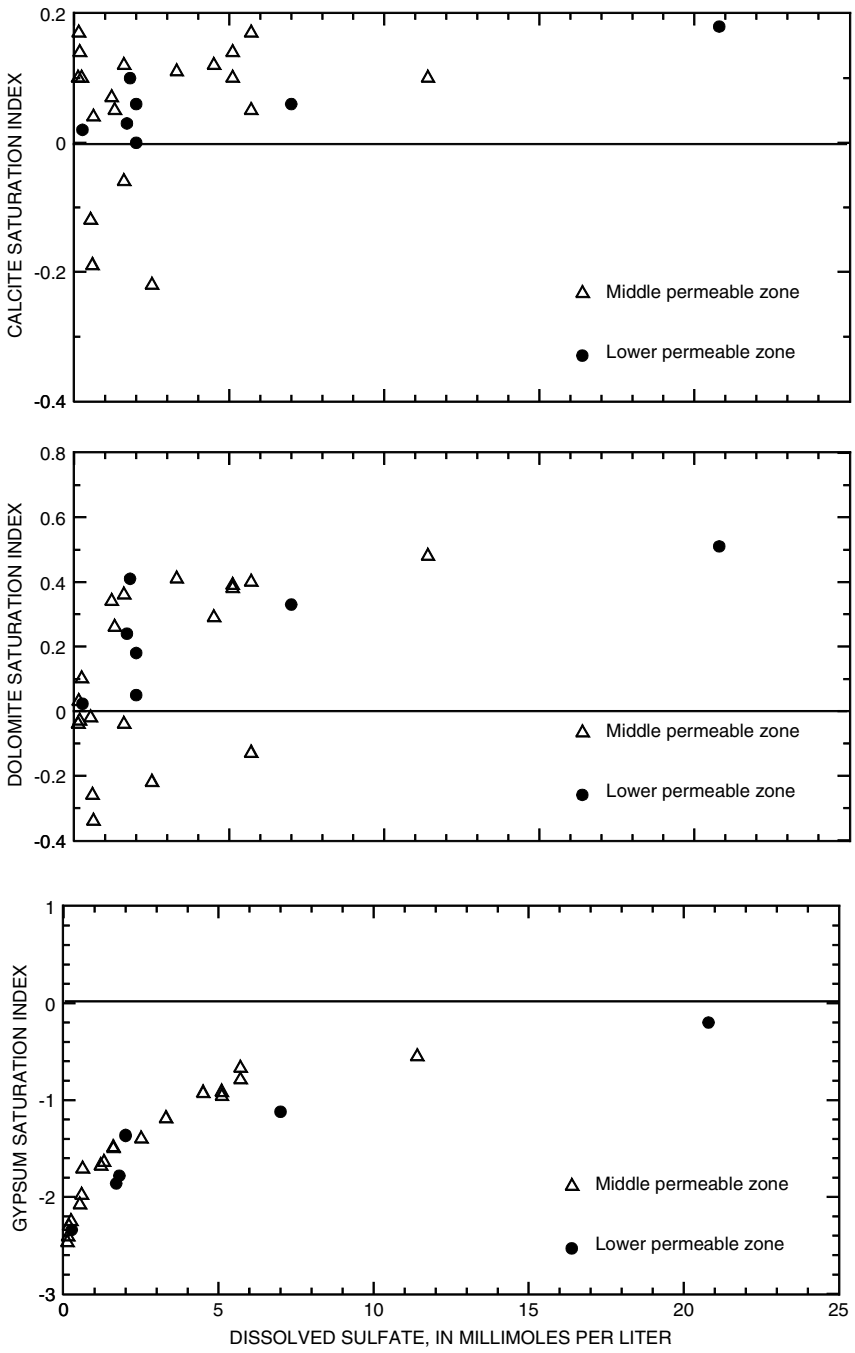

Figure 8. Relation of calcite, dolomite, and gypsum saturation indices to dissolved sulfate for samples collected from the Trinity aquifer, south-central Texas.

radioactive decay is not the only process which contributes to the change in ^{14}C composition along a flowpath. Geochemical reactions involving the exchange of carbon between the solid phase containing no ^{14}C and the aqueous phase will dilute the amount of ^{14}C in the aqueous phase. Thus, it is necessary to adjust ^{14}C activity for chemical reactions other than radioactive decay along a flowpath using the carbon mass balance from NETPATH.

NETPATH uses three values of ^{14}C concentration (pmc) to calculate travel time: (1) measured ^{14}C (table 5) for water in upgradient well, A_o; (2) calculated

Table 6. Results from NETPATH modeling

[For calculated mass-transfer results, negative number indicates amount of mineral precipitating, positive number indicates amount of mineral dissolving. For exchange, negative number indicates milliequivalents calcium exchanged from solid to aqueous phase, positive number indicates milliequivalents sodium exchanged from aqueous to solid phase. For CO_2 gas, negative number indicates degassing, positive number indicates CO_2 gas being dissolved. <, less than; >, greater than]

Flow-path	Mass transfer (mmol/L)						$\delta^{13}C$ (‰)		^{14}C activity (pmc)		Adjusted ^{14}C travel time (years)
	Calcite	Dolomite	Gypsum	Sodium chloride	Exchange	CO_2 gas	Calculated	Measured	Calculated[1]	Measured	
1	-8.07	4.25	5.74	0.46	0.67	-0.14	-1.8	-1.82	6.5	1.2	14,000
2	-1.09	.41	.001	9.58	-1.11	.23	-7.8	-7.7	1.4	<.4	>10,000

[1] Corrected for reaction effects but not radioactive decay.

(adjusted) ^{14}C for water in downgradient well, A_{nd}; and (3) measured ^{14}C (table 5) for water in downgradient well, A. A_{nd} is calculated by NETPATH using A_o, defined ^{14}C isotopic content of carbon sources, defined ^{14}C fractionation factors, and calculated carbon mass transfer (Plummer and others, 1991). Chemical reactions account for the change between ^{14}C composition between A_o and A_{nd} (usually a decrease). Radioactive decay accounts for the difference between A_{nd} and A. The calculated A_{nd} is 6.5 pmc for flowpath 1and 1.4 pmc for flowpath 2. Using these values in the following equation (Plummer and others, 1991) yields travel time between wells:

$$\Delta t = \frac{5,730}{\ln 2} \ln\left(\frac{A_{nd}}{A}\right), \qquad (7)$$

where

Δt is travel time, in years, between upgradient and downgradient wells; and A_{nd} and A are as defined above.

Calculated A_{nd} for flowpath 1 is 6.5 pmc. The travel time calculated by NETPATH for water in the middle permeable zone to flow along flowpath 1 from upgradient well 18 to downgradient well 23 is about 14,000 years. Using this travel time and a distance of 4.4 miles (mi) between the wells, a ground-water velocity of about 1.7 feet per year (ft/yr) is computed.

Calculated A_{nd} for flowpath 2 is 1.4 pmc. The travel time for water in the lower permeable zone to flow along flowpath 2 from upgradient well 2 to downgradient well 12 could be determined only as a lower limit because ^{14}C was below the detection limit at well 12. The resulting time is at least 10,000 years. Using this travel time and a distance of 8.3 mi between the wells, a ground-water velocity of less than 4.4 ft/yr is computed.

A regional ground-water-flow simulation (E.L. Kuniansky, U.S. Geological Survey, written commun., 1993) calculated velocities ranging from 3 to 4 ft/yr in the vicinity of flowpath 1 and from 2 to 6 ft/yr in the vicinity of the flowpath 2. These velocities are based on an overall porosity of 16 percent. Hammond (1984) also used 16-percent porosity to compute flow velocities in the lower Glen Rose Limestone (upper part of middle permeable zone). Hammond (1984) computed higher flow velocities, ranging from 13.8 to 16.1 ft/yr.

SUMMARY

The chemistry of water in the Trinity aquifer in south-central Texas is different for each of three permeable zones and also varies by geographical location. The upper permeable zone generally yields small quantities of water to wells but was not included in this study. The middle permeable zone primarily comprises limestone and dolostone. The lower permeable zone lithology is clastic sand, marine limestone, and dolostone. The dissolved solids concentrations of water generally are greater in the lower permeable zone than in the middle permeable zone. Dissolved solids concentrations in samples from 19 wells in the middle permeable zone and 7 wells in the lower permeable zone range from 329 to 1,820 mg/L and from 518 to 3,030 mg/L, respectively. Hydrochemical facies in the middle permeable zone principally are calcium magnesium bicarbonate

and calcium magnesium sulfate. Hydrochemical facies in the lower permeable zone are variable. In the southeastern part of the study area, tritium concentrations range from 4.7 to 5.3 TU at wells 10, 11, 24, and 26. These concentrations indicate the presence of relatively recent recharge water. Trilinear diagram analyses of chemical data, equilibrium calculations, and mass-transfer simulations indicate that a principal geochemical process in the middle permeable zone of the Trinity aquifer is dedolomitization. Processes in the lower permeable zone include sodium chloride dissolution, dedolomitization, and cation exchange between the solid and aqueous phases. Results from simulation along flowpath 1 in the middle permeable zone show a mass transfer of 4.25 mmol/L of dolomite dissolved, 5.74 mmol/L of gypsum dissolved, and 0.46 mmol/L sodium chloride dissolved; 8.07 mmol/L of calcite precipitated; and 0.67 mmol/L of calcium-for-sodium cation exchange between solid and aqueous phases. Results from simulation along flowpath 2 in the lower permeable zone show mass transfer of 0.41 mmol/L of dolomite dissolved, 0.001 mmol/L of gypsum dissolved, and 9.58 mmol/L sodium chloride dissolved; 1.09 mmol/L of calcite precipitated; and 1.11 mmol/L of sodium-for-calcium cation exchange between solid and aqueous phases. Ground-water travel times also were calculated using NETPATH, and flow velocities computed. The time for water to flow along the 4.4-mi flowpath 1 in the middle permeable zone is about 14,000 years, which results in a velocity of 1.7 ft/yr. The time for water to flow along the 8.3-mi flowpath 2 in the lower permeable zone is at least 10,000 years, which results in an estimated velocity of less than about 4.4 ft/yr.

SELECTED REFERENCES

Achauer, C.A., 1977, Contrasts in cementation, dissolution, and porosity development between two Lower Cretaceous reefs of Texas, *in* Bebout, D.G., and Loucks, R.G., eds., Cretaceous carbonates of Texas and Mexico—Applications to subsurface exploration: Austin, University of Texas, Bureau of Economic Geology Report of Investigation 89, p. 127–135.

Amsbury, D.L., 1974, Stratigraphic petrology of Lower and Middle Trinity rocks on the San Marcos platform, south-central Texas, *in* Perkins, D.F., ed., Aspects of Trinity division geology—A symposium: Louisiana State University, Geoscience and Man, v. 8, p. 1–35.

Anderson, T.F., and Arthur, M.A., 1983, Stable isotopes of oxygen and carbon and their application to sedimentologic and paleoenvironmental problems, *in* Arthur, M.A., and others, eds., Stable isotopes in sedimentary geology: Dallas, Society for Sedimentary Geology short course no. 10.

Ashworth, J.B., 1983, Ground-water availability of the Lower Cretaceous formations in the Hill Country of south-central Texas: Texas Department of Water Resources Report 273, 173 p.

Barker, R.A., and Ardis, A.F., 1992, Configuration of the base of the Edwards-Trinity aquifer system and hydrogeology of the underlying pre-Cretaceous rocks, west-central Texas: U.S. Geological Survey Water-Resources Investigations Report 91–4071, 25 p.

_____1996, Hydrogeologic framework of the Edwards-Trinity aquifer system, west-central Texas: U.S. Geological Survey Professional Paper 1421–B, 61 p.

Busby, J.F., Plummer, L.N., Lee, R.W., and Hanshaw, B.B., 1991, Geochemical evolution of water in the Madison aquifer in parts of Montana, South Dakota, and Wyoming: U.S. Geological Survey Professional Paper 1273–F, p. F16.

Bush, P.W., Ulery, R.L., and Rittmaster, R.L., 1994, Dissolved-solids concentrations and hydrochemical facies in water of the Edwards-Trinity aquifer system, west-central, Texas: U.S. Geological Survey Water-Resources Investigations Report 93–4126, 29 p.

Claassen, H.C., 1982, Guidelines and techniques for obtaining water samples that accurately represent the water chemistry of an aquifer: U.S. Geological Survey Open-File Report 82–1024, 49 p.

Dansgaard, W., 1964, Stable isotopes in precipitation: Tellus, v. 16, p. 436–468.

Domenico, P.A., and Schwartz, F.W., 1990, Physical and chemical hydrology: New York, Wiley, 824 p.

Drever, J.I., 1988, The geochemistry of natural waters: Englewood Cliffs, N.J., Prentice Hall, 437 p.

Fritz, P., and Fontes, J.C., eds., 1980, Handbook of environmental isotope geochemistry, v. 1, The terrestrial environment, A: Amsterdam, Elsevier, 545 p.

Hammond, W.W., Jr., 1984, Hydrogeology of the lower Glen Rose aquifer, south-central Texas: Austin, University of Texas, Ph.D. dissertation, 245 p.

Hanshaw, B.B., and Back, W., 1979, Major geochemical processes in the evolution of carbonate-aquifer systems, *in* Back, W., and Stephenson, D.A., eds., Contemporary hydrogeology—The George Burke Maxey memorial volume: Journal of Hydrology, v. 43, p. 290.

Hem, J.D., 1985, Study and interpretation of the chemical characteristics of natural water (3d ed.): U.S. Geological Survey Water-Supply Paper 2254, 263 p.

Hoefs, J., 1987, Stable isotope geochemistry (3d ed.): New York, Springer-Verlag, 241 p.

Hutchinson, C.S., 1974, Laboratory handbook of petrographic techniques: New York, Wiley, 527 p.

Kuniansky, E.L., 1990, Potentiometric surface of the Edwards-Trinity aquifer system and contiguous hydraulically connected units, west-central Texas, winter 1974–1975: U.S. Geological Survey Water-Resources Investigations Report 89–4208, 2 sheets.

Kuniansky, E.L., and Holligan, K.Q., 1994, Simulations of flow in the Edwards-Trinity aquifer system and contiguous hydraulically units, west-central Texas: U.S. Geological Survey Water-Resources Investigations Report 93–4039, 40 p.

Maclay, R.W., and Small, T.A., 1984, Carbonate geology and hydrology of the Edwards aquifer in the San Antonio area, Texas: U.S. Geological Survey Open-File Report 83–537, 72 p.

Perkins, B.F., 1974, Paleoecology of a rudist reef complex in the Comanche Cretaceous Glen Rose Limestone of central Texas, *in* Perkins, D.F., ed., Aspects of Trinity division geology—A symposium: Louisiana State University, Geoscience and Man, v. 8, p. 131–173.

Petta, T.J., 1977, Diagenesis and geochemistry of a Glen Rose patch reef complex, Bandera County, Texas, *in* Bebout, D.G., and Loucks, R.G., eds., Cretaceous carbonates of Texas and Mexico—Applications to subsurface exploration: Austin, University of Texas, Bureau of Economic Geology Report of Investigation 89, p. 138–165.

Plummer, L.N., Jones, B.F., and Truesdell, A.H., 1976, WATEQF—A FORTRAN IV version of WATEQ, a computer program for calculating chemical equilibria of natural waters: U.S. Geological Survey Water-Resources Investigations Report 76–13, 61 p.

Plummer, L.N., Prestmon, E.C., and Parkhurst, D.C., 1991, An interactive code (NETPATH) for modeling net geochemical reactions along a flow path: U.S. Geological Survey Water-Resources Investigations Report 91–4078, 227 p.

Rose, P.R., 1972, Edwards Group, surface and subsurface, central Texas: Austin, University of Texas, Bureau of Economic Geology Report of Investigation 74, 198 p.

Stricklin, F.L., Jr., and Smith, C.I., 1973, Environmental reconstruction of a carbonate beach complex, Cow Creek (Lower Cretaceous) Formation of central Texas: Geological Society of America Bulletin v. 84, no. 4, p. 1,349–1,367.

Stricklin, F.L., Jr., Smith, C.I., and Lozo, F.E., 1971, Stratigraphy of Lower Cretaceous Trinity deposits of central Texas: University of Texas at Austin, Bureau of Economic Geology Report of Investigation 71, 63 p.

Sun, R.J., ed., 1986, Regional Aquifer-System Analysis program of the U.S. Geological Survey—Summary of projects, 1978–84: U.S. Geological Survey Circular 1002, 264 p.

Taggart, J.E., Jr., Lindsay, J.R., Scott, B.A., Vivit, D.V., Bartel, A.J., and Stewart, K.C., 1987, Analysis of geologic materials by wavelength dispersive X-ray fluorescence spectrometry, Chapter E: U.S. Geological Survey Bulletin 1770, p. E1–E19.

Walker, L.E., 1979, Occurrence, availability, and chemical quality of ground-water in the Edwards Plateau region of Texas: Texas Department of Water Resources Report 235, 336 p.

Wood, W.W., 1976, Guidelines for collection and field analysis of ground water samples for selected unstable constituents: U.S. Geological Survey Techniques of Water-Resources Investigations, book 1, chap. D2, 24 p.